THE ASTROPHYSICAL JOURNAL, 301:331–338, 1986 February 1

ZEEMAN SPLITTING OF 18 CENTIMETER OH LINES TOWARD CASSIOPEIA A AND OTHER SOURCES

CARL HEILES AND MARY STEVENS
Astronomy Department, University of California, Berkeley
Received 1985 January 11; accepted 1985 July 16

ABSTRACT

We have detected Zeeman splitting of the OH absorption lines toward Ori B, W22, and Cas A. For W22, the derived magnetic field strength is -11 μG. For Ori B, the inferred magnetic field strength is consistent in magnitude, but not in direction, with the 38 μG derived previously by Crutcher and Kazes; the field is positive and therefore points away from the observer.

For Cas A, the average field in four velocity components is $+9$ μG, in the same direction as, but weaker than, the field strengths measured in single-dish H I data. They are considerably weaker than the field strengths in less dense H I clumps that are associated with the OH clumps. This circumstance raises serious interpretive difficulties.

Subject headings: interstellar: magnetic fields — interstellar: molecules — nebulae: individual — Zeeman effect

I. INTRODUCTION

Radio astronomers in the northern hemisphere are fortunate because they can observe the strongest radio continuum source in the sky, Cas A. This source is particularly interesting because the line of sight intersects a dense group of atomic and molecular clouds in the Perseus arm. Many studies of these clouds have contributed substantially to our understanding of interstellar matter (see review by Troland, Crutcher, and Heiles 1985).

Cas A was the first direction in which Zeeman splitting of the H I line was detected (Verschuur 1969). There are two H I velocity components in the Perseus arm absorption feature; they have field strengths of 11 and 18 μG. Recent work on Cas A (Bregman *et al.* 1983; Schwarz *et al.* 1985) has used aperture synthesis to map the field, and field strengths of up to ~ 40 μG have been measured in the H I line near molecular clumps that cover portions of the source.

OH lines also appear in absorption against Cas A. Nature has therefore presented us with a unique opportunity to compare directly the field strengths in a molecular region with those in an adjacent, less dense atomic region.

The 18 cm OH lines are the best molecular lines for detecting Zeeman splitting in molecular clouds because of their low frequency and large Landé g-factors. In this paper, we report the detection of OH Zeeman splitting in three sources and upper limits for seven others. Two of the sources, Ori B and W22, have been, or will be, discussed elsewhere (Crutcher and Kazes 1983, 1985), and we do not discuss them in detail here. We concentrate our interpretive discussion on Cas A in § III.

II. OBSERVATIONS

a) Instrumentation and Technique

Observations were performed in five observing periods during the calendar year 1982, plus an additional period during summer 1984, for W67 and the wide-band observations of Sgr A. We used the Hat Creek 85 foot telescope (HPBW = 30′ at 18 cm wavelength) equipped with dual-channel, cooled, field effect transistor amplifiers having system temperatures of ~ 55 K. The polarization transducer is a turnstile junction polarimeter. The polarization switch consists of two motor-driven waveguide shorts, which simultaneously alternate between two positions so as to switch between orthogonal circular polarizations at each receiver port. The spectrometer is a 1024 channel, three-level correlator. The correlator was split into four, 256 channel quadrants, so that both the 1665 and 1667 MHz lines and both polarizations could be observed simultaneously, except for the wide-band Sgr A observations. For these, a bandwidth of 10 MHz was used, which covers both OH lines, so the correlator was split into two, 512 channel halves. Except as noted, all sources were observed with a bandwidth of 0.3125 MHz (channel spacing 0.22 km s^{-1}).

Systematic effects involving circular polarization of the telescope sidelobes and primary beam pattern can be serious for measurements of the Zeeman effect in the 21 cm line (Troland and Heiles 1982). However, these effects do not affect the present observations. For the OH lines in absorption, the continuum source is much smaller than the telescope beam, so these effects are unimportant. For the OH lines in emission, the sensitivity is so poor that these systematic effects are negligible. For observations of Sgr A, the most serious potential instrumental effect is beam displacement of the two circular polarizations. This was minimized by using the procedures described by Troland and Heiles (1982).

Another instrumental effect arises from the difference in system gains between the two polarization switch positions. This causes a scaled-down replica of the line profile to appear in the V spectrum. Troland and Heiles (1982) described the usual scheme to bypass this problem, which involves a least-squares fit of the V spectrum to two terms involving the I spectrum and its derivative. However, this method is intrinsically unsatisfactory because it implicitly assumes that the line itself has zero circular polarization. This assumption is particularly unsatisfactory for the OH lines, which are often circularly polarized.

We have employed a new method to eliminate gain differences from the V spectrum. We have determined that nearly all of the effect arises because of the difference between the receiver gains, which depends slowly on frequency and typically varies from 3% to 4% or so across our typical measured passband of a few hundred kHz. In contrast, the difference between the telescope gains is smaller than 0.1%. Thus, the ratio of the system gains in the two polarizations is essentially equal to the ratio of the receiver gains. In this case, it is easy to show that the ratio of the system gains is simply equal to the ratio of the uncalibrated spectra in the two polarizations. To an accuracy of 0.1%, no replica of the line profile appears in this "ratio spectrum."

This happy situation allows us to determine the system gain ratio by least-squares fitting a low-order polynomial to the entire ratio spectrum. The entire spectrum, not just that portion containing the spectral line is used; furthermore, the line itself does not appear in the ratio spectrum, as long as it is not highly polarized itself. If it is thought to be polarized, it can be excluded from the fit. Thus, the determination of this instrumental effect is entirely independent of the properties of, or even the existence of, the spectral line.

After this correction for the system gain difference, the V spectrum contains no further instrumental effects. In deriving magnetic field strengths, this allowed us to least-squares fit the V spectrum to only the derivative of the I spectrum; we did not need to account for presence of a scaled-down replica of the I spectrum itself.

For sources other than Cas A, the overall intensity calibration is accurate to only $\sim$30%. A broad-band calibration signal was radiated from the vertex by a small, linearly polarized antenna. This limited our accuracy, because such a radiated signal has standing waves between the paraboloid and the feed, which cause the apparent intensity of the signal to vary strongly with frequency. Changes in the distance between the feed and the vertex occur because of thermal expansion and gravitational deformation and move the standing wave pattern with respect to the observed bandpass. This caused the apparent intensity of the calibration source to change erratically with time. Even though the overall intensity calibration is uncertain, the relative calibration between I and V spectra is exact, because precisely the same data were used to construct both spectra.

b) Results for Sources Other than Cas A

Ten sources were observed; the results, as discussed by the technique described above, are summarized for all sources but Cas A in Table 1. An error in the on-line Doppler correction prevented us from deriving the exact LSR velocities. Where possible, we assumed the velocity scale of Goss (1968) to be correct and aligned our spectra accordingly; elsewhere we estimated the approximate errors involved and corrected the velocities accordingly. Ori B, W22, W67, Sgr A, M17, and Cas A exhibit the OH line in absorption; the remaining positions are dust clouds that show the OH lines in roughly normal thermal emission. Quoted errors are 1 σ; 3 σ is a good measure of the strict upper limit for an individual measurement (Troland and Heiles 1982). The circular polarization in Sgr A is nowhere larger than 0.7% of the peak line strength.

Thus, there are two detections in Table 1: Ori B and W22. Derived values of magnetic field strengths are from the average of the 1665 and 1667 MHz spectra. Using an average is reasonable. The Landé g-factor for the 1665 MHz line is 1.67 times larger than that for the 1667 MHz line, while the optical depth of the 1665 MHz line is 1.8 times smaller than that of the 1667 MHz line for thermal excitation conditions, so the V spectra of the two lines should have the same amplitude to within 8%.

Our Ori B spectra, not shown here, look similar to and confirm the first detection of circular polarization by Verschuur and Turner (1970) in this source and also confirm the spectra of Crutcher and Kazes (1983), whose sensitivity is much better than ours. However, Crutcher and Kazes incorrectly stated the sense of the magnetic field. The magnetic field seen in absorption against Ori B is actually positive, pointing away from the observer.

Figure 1 shows the results for W22. These spectra were orig-

TABLE 1

Derived Magnetic Field Strengths

Source	R.A.(1950)	Decl.(1950)	LSR Velocity (km s^{-1})	B (1 σ errors) (μG)
Dust cloud	05:34:21	−06:38:40	+7	−28 ± 17
Dust cloud	05:37:01	−07:31:26	+8	−3 ± 11
Ori B (NGC 2024)	05:38:58	−01:53:57	+9	+38 ± 2[a]
L134	15:51:00	−04:32:00	+3	+3 ± 8
L183	15:51:33	−02:46:24	+2	−2 ± 17
W22 (NGC 6357)	17:22:11	−34:17:06	−3	+4 ± 14
W22 (NGC 6357)	17:22:11	−34:17:06	+6	−11.0 ± 2.2
Sgr A (narrow)[b]	17:42:18	−28:58:04	−50	+6 ± 8
Sgr A (narrow)[b]	17:42:18	−28:58:04	−30	+1 ± 6
Sgr A (narrow)[b]	17:42:18	−28:58:04	0	+8 ± 5
Sgr A (wide)[b]	17:42:18	−28:58:04	−125	+60 ± 106
Sgr A (wide)[c]	17:42:18	−28:58:04	+40	+8 ± 19
W38 (M17)	18:17:47	−16:19:06	+20	−14 ± 14[c]
W67 (DR 5)	20:25:35	39:53:04	+1	1 ± 5

[a] From Crutcher and Kazes 1983, but with sign reversed (*see text*).

[b] Narrow-band spectra of Sgr A were taken with total bandwidth 625 kHz, channel spacing 2.44 kHz, to cover the three listed narrow-velocity components in detail. Wide-band spectra were taken with total bandwidth 10 MHz, channel spacing 19.5 kHz to cover the two listed broad velocity components (see Palmer and Zuckerman, 1967, for the Sgr A OH line profile).

[c] Complex line shape. Magnetic field limit applies to sharp positive-velocity edge. Polarized maser emission in 1665 MHz line prevented including it in average for magnetic field determination.

1986ApJ...301..331H

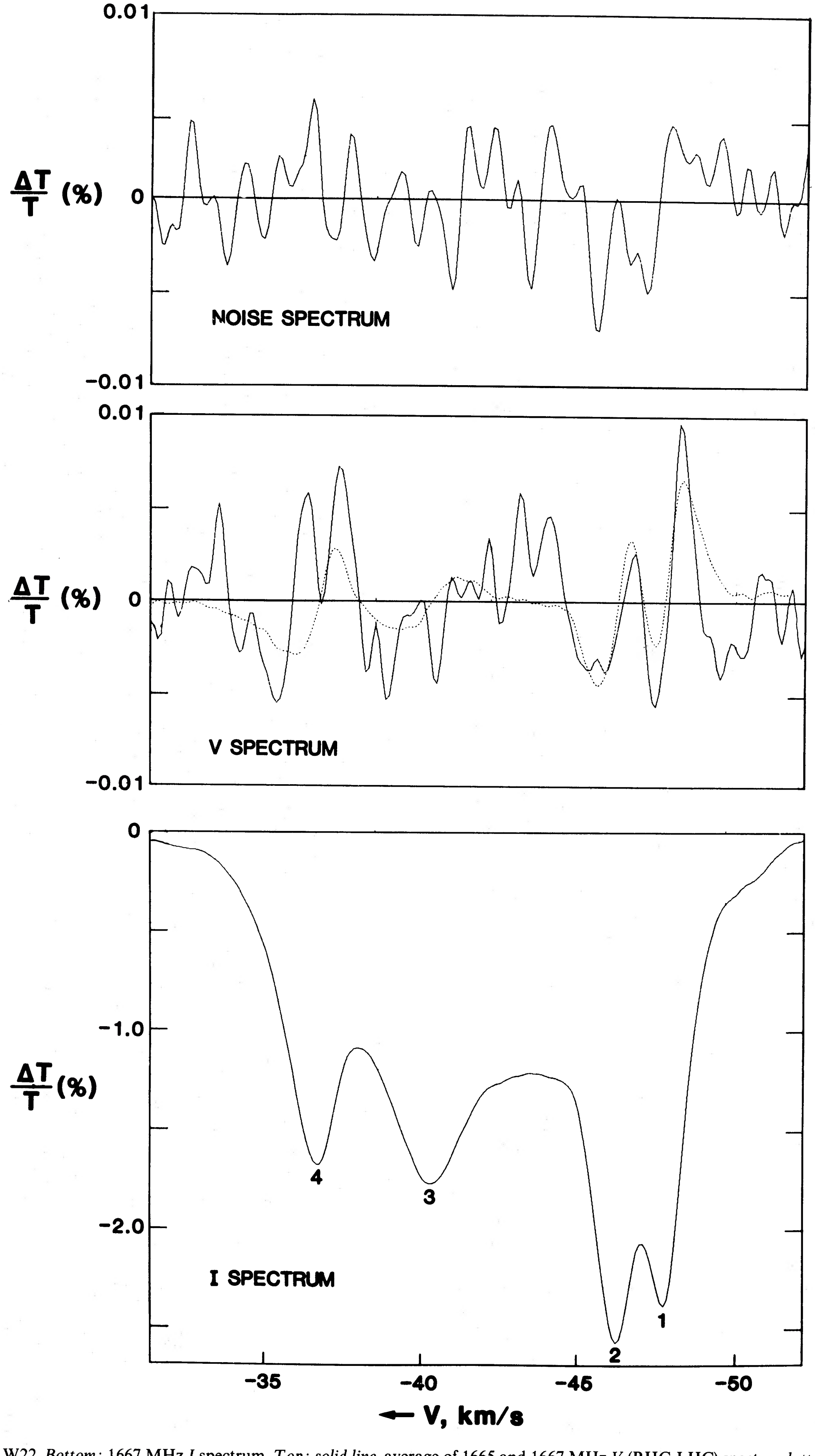

FIG. 1.—Results for W22. *Bottom:* 1667 MHz *I* spectrum. *Top: solid line*, average of 1665 and 1667 MHz *V* (RHC-LHC) spectra; *dotted line*, Zeeman pattern for $B = -11.0$ μG. Zeeman splitting detection of -11 μG, reported in Table 1, refers *only* to the narrow absorption component centered $\sim +6$ km s^{-1}. The negative-going spike in the *V* spectrum centered near -2 km s^{-1} is probably a weak, polarized maser.

inally obtained with a resolution of 0.22 km s^{-1}, but were smoothed to 0.44 km s^{-1}. The *I* spectrum, in the bottom panel, exhibits two distinct velocity components. The *V* spectrum, in the top panel, is shown by a solid line. It is the average of the 1665 MHz and 1667 MHz *V* spectra. The dotted line superposed on the *V* spectrum is the frequency derivative of the *I* spectrum, scaled to the derived field of -11 μG. The Zeeman detection refers *only* to the narrow component centered $\sim +6$ km s^{-1}. The negative-going spike ~ -2 km s^{-1} is probably a weak, polarized maser, and the broad absorption line exhibits no detectable Zeeman splitting.

Crutcher and Kazes (1985), using the Nançay telescope, have also measured the OH Zeeman splitting of the narrow component against W22. They derive a magnetic field of -18.2 μG with a small error. Our two measurements probably do not agree within the formal errors. In addition, they do not see the maser. These differences are almost certainly a result of their higher angular resolution, because the source is larger than their beamwidth. Crutcher and Kazes (1985) have made CO measurements in this region and determined that the OH absorption line arises from a dark cloud with an H_2 volume density of ~ 1000 cm^{-2} and a temperature of ~ 10 K.

c) *Results for Cas A*

Figure 2 shows the results for Cas A, which required a total of 304 hr of integration time. All spectra were originally obtained with a resolution of 0.11 km s^{-1}, but were smoothed to a resolution of 0.44 km s^{-1} during the data reduction. The *I* spectrum for the 1667 MHz line is shown in the bottom panel. The *I* spectrum exhibits four distinct velocity components, to which we shall refer by the numbers 1–4, as denoted on the figure.

Both the shape and overall depth of the Cas A OH absorption spectrum have apparently changed over the years. We have not tried to determine whether these changes are real or instrumental. Real changes might occur because of the expansion of Cas A, which amounts to $\sim 0.3\%$ per year. Instrumental effects might occur because Cas A is such a strong radio source and possibly because its angular size is not totally negligible compared to single-dish beamwidths. Two previously published spectra with adequate frequency resolution, taken with single telescopes having beamwidths larger than Cas A, show significant differences. The least ambiguous change appears in the intensity ratio of the 0 km s^{-1} "Orion arm" component to our component number 2. Measuring line intensities directly from the published line profiles instead of using Gaussian-fitted components, we find this ratio to be ~ 1.03 and 1.17 for Goss (1968) and Davies and Matthews (1972), respectively. In two separate sets of observations, one taken in summer 1984 and the other in spring 1985, we find the ratio to be ~ 0.89. There also seem to be other more subtle differences between the relative intensities, within both the Orion arm and Perseus arm components themselves.

Apart from these differences in line shape, there are also differences in the overall optical depth scale. These are probably instrumental errors, because it is hard to imagine that the overall optical depth scale has changed significantly. For the Perseus arm components, the scales of Goss (1968) and Davies and Matthews (1972) are in approximate agreement. In contrast, our optical depths are smaller by a factor of ~ 1.4; those in the discovery papers (Weinreb *et al.* 1963; Barrett, Meeks, and Weinreb 1964) are even smaller. We made a special series of measurements during spring 1985 to determine accurately the optical depth scale; the scale shown in Figure 2 is accurate to $\sim 5\%$. This appears to be consistent with the scale of de Jager *et al.* (1978), who have too much angular resolution for an accurate comparison.

The *V* spectrum, actually the average of the 1665 and 1667 MHz *V* spectra, is shown by the solid line in the middle panel of Figure 2. The dashed line is the frequency derivative of the *I* spectrum, scaled for illustrative purposes to a field strength of $+9$ μG. This value was chosen because it is the average for the four velocity components, as discussed below.

There is good correspondence between the solid and dashed lines in Figure 2, particularly given the low signal-to-noise ratio. This shows that we have detected Zeeman splitting. We least-squares fit the *V* spectrum to derive the field strengths separately for each of the four velocity components using a velocity range covering the full extent of each component. The results are given in Table 2. Quoted errors are 1 σ. Within the errors, the derived fields strengths are all the same; the average is 9 μG. For OH components 1 and 2, the derived values are considerably larger than the errors. This is less so for component 3, and for component 4 the derived value is only barely significant compared to the error. This is particularly evident in Figure 2. The large uncertainty in component 4 is not surprising because the signal-to-noise ratio in the *V* spectrum is low and component 4 is the weakest.

III. THE PHYSICAL ENVIRONMENT IN CAS A

a) *Morphology of Molecular and Atomic Gas*

The angular distribution of the OH absorption has been mapped with the VLA by Bieging and Crutcher (1984). Unfortunately, their data have not yet been fully analyzed. However, the overall characteristics of the OH distribution mimic those of the H_2CO in most, but not all, respects. The H_2CO distribution has been discussed in detail by Goss, Kalberla, and Dickel (1984) using WSRT observations.

The H_2CO is distributed in 16 "clumps" (in the terminology of Goss *et al.* 1984), localized in both space and velocity. On the basis of velocity, most of these clumps can be associated with the four OH line components, as shown in Table 3. Four clumps have velocities that do not correspond with the OH component velocities and must be too small to produce individual components in the single-dish OH spectrum. None of these clumps is more massive than 1 $M_\odot$, and all are located near the western periphery. Three of these, VI, VII, and VIII, are centered ~ -43 km s^{-1}; the fouth, IV, is centered at -47.3 km s^{-1} and is unique among the more negative-velocity clumps in being located at the western periphery.

The molecular clouds are associated with small H I features detected in 21 cm line absorption maps made with the WSRT (Kalberla, Schwarz, and Goss 1985). The H I features are difficult to discern because they contribute only a small amount to

TABLE 2

Magnetic Field Strengths in OH Absorption against Cas A

OH Component	LSR Velocity (km s^{-1})	Magnetic Field (1 σ errors) (μG)
1.........	-48	$+8.3 \pm 1.6$
2.........	-46	$+7.9 \pm 0.7$
3.........	-41	$+11.1 \pm 2.8$
4.........	-37	$+8.3 \pm 2.9$

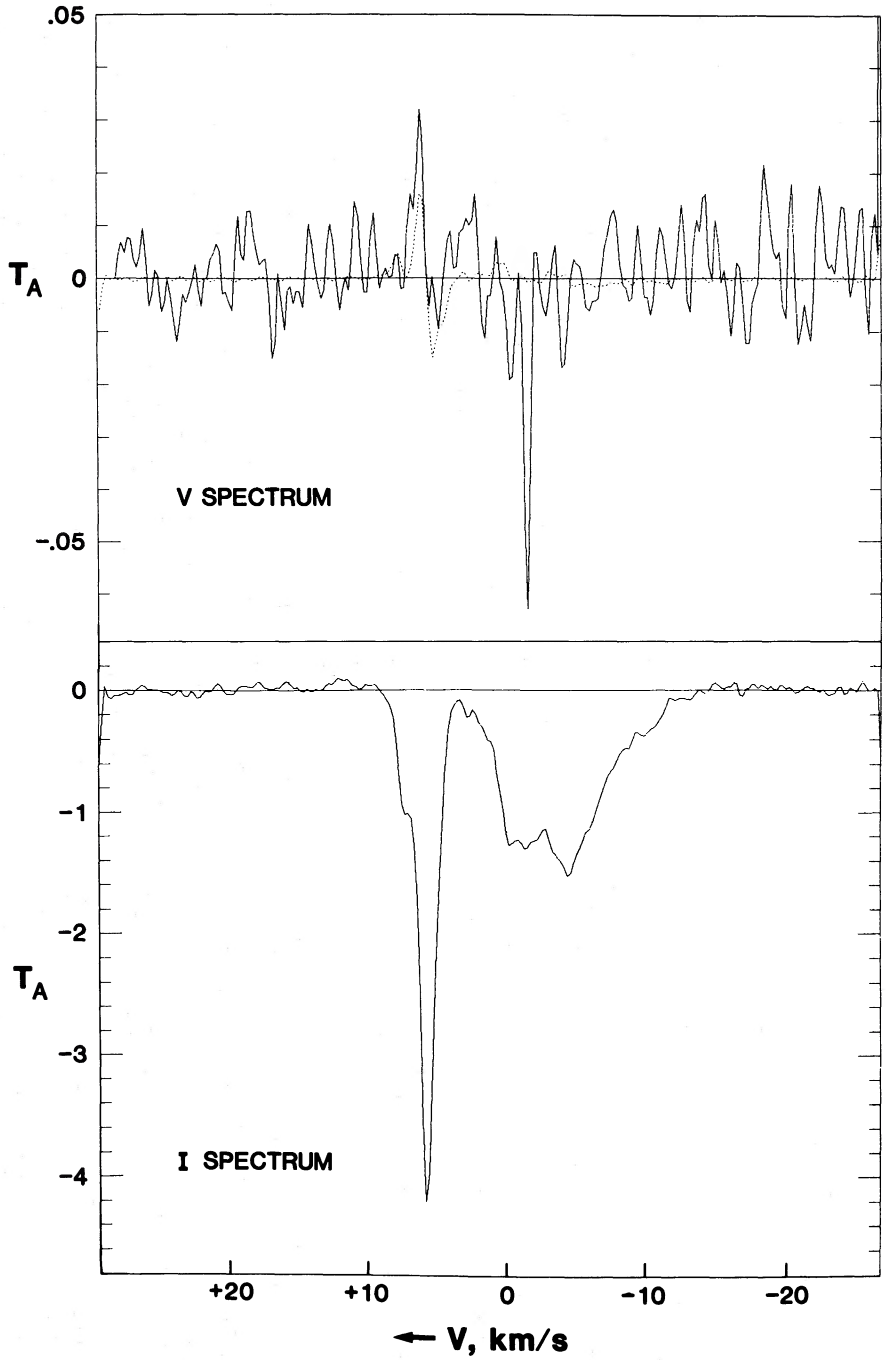

FIG. 2.—Results for Cas A. *Bottom*: 1667 MHz *I* spectrum; the four velocity components are numbered in order of increasing velocity, as they are referred to in text. *Middle: solid line*, average of 1665 and 1667 MHz V spectra; *dotted line*, expected Zeeman pattern for $B = 9\ \mu$G, equal to the average of the four components listed in Table 2. *Top:* half of the difference between the 1667 and 1665 MHz *V* spectra, presented to illustrate the character of the noise. Optical depth scale is accurate to 5%.

the total absorption, and the background H I optical depths are large. In fact, for $v < -46$ km s^{-1} (our OH components 1 and 2), the background optical depths are so large as to obscure excess H I absorption by small H I features. All of the molecular clumps having $v > -46$ km s^{-1} are associated with excess H I, so it seems reasonable to assume that all clumps with $v < -46$ km s^{-1} are also associated with excess H I.

The H I associated with the molecular clumps has larger angular sizes than the clumps themselves. Goss *et al.* (1984) assumed that the H I is distributed in shells that surround the clumps; as discussed below in § IIIc, the term "shell" may conjure an incorrect mental image. The typical mass of an H I "shell" is 1 $M_{\odot}$ and the typical volume density is 350 cm^{-3}. The central velocities of the H I "shells" are not exactly equal to those of the associated molecular clumps and in one extreme case differ by 2.7 km s^{-1}. However, the H I central velocities, as well as the other derived parameters, have large errors because the H I optical depths are so large.

TABLE 3

ASSOCIATION BETWEEN OH VELOCITY COMPONENTS AND H_2CO CLUMPS

OH Component	LSR Velocity (km s^{-1})	Clump[a]	Mass ($M_\odot$)	Locale in Cas A Map
1.........	−48	I	0.06	
		II	0.6	southeastern periphery
		III	2.2	
2.........	−46	V	5.4	southern periphery
3.........	−40	IX	3.3	
		X	>3.6	
		XI	>19.8	string extending from
		XII	1.4	center to western periphery
		XIII	3.9	
4.........	−37	XIV	3.3	
		XV	0.8	southwestern periphery
		XVI	0.8	

[a] From Goss *et al.* 1984; our quoted masses are 3.3 times smaller than theirs (*see* § III*b*).

The masses of the H I "shells" are comparable to those of the H_2 clumps, while the volume densities are ~ 6 times smaller. All of the molecular clumps but XI have masses smaller than 3.6 $M_\odot$. With H I "shells" of ~ 1 $M_\odot$, the molecular clumps are typically only a bit more massive than their H I "shells"—and, given the uncertainties, the molecular and atomic masses could typically be equal.

b) H_2 *Volume Densities*

It is often stated that the magnetic field strength increases with volume density in astronomical objects. Thus, we wish to know the H_2 density in the molecular clumps.

Published estimates vary and may reflect real variations because of clumping. The highest estimates, which range up to 5×10^4 cm^{-3}, are obtained by Batrla, Wilson, and Martin-Pintado (1983). These are based on observations of the 5.6 and 14.5 GHz transitions of H_2CO and the use of the excitation calculations of Henkel, Walmsley, and Wilson (1980). Lower values ranging from 10^3 to 10^4 cm^{-3} are derived by Troland, Crutcher, and Heiles (1985), using observations of the 2–1 and 1–0 CO lines, seen in emission against Cas A, and the large velocity gradient excitation model of Goldsmith, Young, and Langer (1983). Troland *et al.* (1985) suggest that the Perseus arm components lie near the lower end of the density range. Values ranging from 5×10^3 to 10^4 cm^{-3} are derived by Batrla, Walmsley, and Wilson (1984) from observations of NH_3 in absorption, using the excitation program of Walmsley and Ungerechts (1983).

Volume densities can be derived more directly from observational data when the angular resolution is high enough to resolve individual clouds and when, in addition, the column density is known, by making the straightforward assumption that the cloud is roughly spherical. This is the method used by Goss *et al.* (1984). They identified a total of 16 H_2CO clumps. They drived H_2 column densities by using a standard ratio of H_2CO to H_2. They obtained values of $\sim 10^4$ cm^{-3}. However, the value of the ratio of H_2CO to H_2 that they used is uncertain, and probably too small. They followed Batrla *et al.* (1983) and used the smallest value compiled by Sherwood and Wilson (1981), who summarized data on H_2CO column density and optical extinction for four dust clouds. However, this smallest value is five times smaller than the average value for the four clouds.

If a value nearer to the average had been used instead, Goss *et al.* (1984) would have obtained typical volume densities of 3×10^3 cm^{-3}. This is the value suggested by Troland *et al.* (1985) and is only somewhat lower than the values derived by Batrla, Walmsley, and Wilson (1984). We adopt these revised values of Goss *et al.* (1984) in the remainder of this paper; they should be relevant to the OH-containing regions to which our measurements refer.

c) *Absence of Virial Equilibrium*

We briefly consider the virial theorem. We restrict our attention to the immediate region. These clumps are not in virial equilibrium unless either our density estimates are much too small or the clumps contain dense cores that are not revealed by existing observations. Goss *et al.* (1984), using H_2 densities that are 3.3 times larger than those we adopt in § III*b*, find upper limits of two for the ratio of the gravitational to the kinetic virial terms, except for two clumps for which the largest value is seven. These are upper limits because they include thermal energy alone; the observed lines are much wider than the thermal width. Thus, because both the H_2 densities are probably lower and the kinetic energy larger than they used in their calculations, the gravitational terms are almost certainly negligible. Surface pressure terms are also negligible (Troland *et al.* 1985).

We conclude that these molecular clumps are evolving dynamically. For example, they may be transient results of a passing shock front. This means that the term "clump" is indeed appropriate, because it does not imply stability as does the term "cloud." It also means that the term "shell," applied to the H I associated with the clumps, may be misleading because it connotates an onionskin structure. While an onionskin structure is certainly possible for a transient object, it is not necessary. If the molecular clumps were formed by shocks, the gas just behind the shock would be the warmest and least dense; as the gas flowed downstream from the shock, it would cool, grow denser and increase the magnetic field strength, and form molecules (e.g., Field *et al.* 1968). In this case the H I would be upstream from the denser molecular regions. The words "transition region," rather than the word "shell," would have the correct connotation.

Given our uncertainty of the correct situation, the word "clump" seems eminently appropriate for the H I regions as well as the molecular regions. We shall use this term henceforth in the present paper.

IV. TOTAL FIELD STRENGTHS IN THE MOLECULAR AND ATOMIC CLUMPS

Angular structure of the magnetic field in the H I has been measured using the WSRT by Bregman *et al.* (1983) and, with higher sensitivity, by Schwarz *et al.* (1985). The measured field strengths range from less than 10 to more than 40 μG. The higher H I field strengths are associated with OH components 2 and 3. In contrast, the H I fields associated with OH components 1 and 4 are not enhanced, having typical values of ~ 14 μG. Thus, the measured fields in the H I clumps associated with OH components 1 and 4 are $\sim 50\%$ higher than the measured fields in the molecular clumps themselves.

The situation for OH components 2 and 3 is more extreme. The parallel components of field strength in their associated H I clumps range from at least 40–60 μG. Thus, typical parallel components of the magnetic field in the H I clumps are ~ 5 times higher than the parallel components in their associated molecular clumps. It is natural to infer that the total field strengths are also larger in the H I clumps.

Such a situation presents a difficulty when viewed in terms of conventional understanding: we might imagine the total field strength in the denser clumps to be *equal* to that in adjacent H I, because of ambipolar diffusion, but there is no way for the molecular clump to *expel* the field and end up with a *smaller* total field than in the adjacent H I.

The field might be tangled so that the total field strength in an OH clump exceeds that in its associated, less dense H I clump. However, this is contrary to theoretical expectation. If the field strength in a molecular clump is equal to the minimum value in the adjacent H I, ~ 50 μG, then the ratio of magnetic to gas pressure is 16 (if $T = 22$ K; Batrla *et al.* 1984). If we instead compare the magnetic pressure to the macroscopic pressure derived directly from the OH line widths (Goss 1968), then the ratio varies from 0.6 to 6. With such ratios of magnetic to gas pressure, the field should not be significantly tangled, at least not so much that the total field strength is enhanced over the systematic component by a factor of 5. We note that the ratio of magnetic to gas pressure in the H I clumps far exceeds that in the molecular clumps, so that the field in the H I clumps can hardly be tangled at all (Schwarz *et al.* 1985).

A remaining possibility is that the ~ 5 times smaller *measured* fields in OH components 2 and 3 are simply a result of a projection effect. Measured field strengths are always lower limits to the total field strengths because Zeeman splitting measurements are sensitive to the parallel (i.e., line-of-sight) component of the magnetic field. If the field is uniform, it is unlikely to point directly along the line of sight, and with a probability of x^{-1} the total field is at least x times the measured field strength (Heiles and Troland 1982). Thus, the factor of 5 reduction occurs with a probability of $\sim \frac{1}{5}$ for each component. But OH components 2 and 3 appear to be independent, because the distributions of their associated H_2CO clumps on the sky are completely different. This implies that the probability that both components suffer the same projection effect is only $\sim 4\%$.

Nevertheless, it is conceivable that OH components 2 and 3 are *not* independent. In § III*c* we concluded that both the atomic and the molecular clumps are transient features. Suppose that clumps 2 and 3, in an initially larger and less dense configuration, were hit by the same passing shock. Suppose, in addition, that they had equal volume densities and were threaded by the same uniform magnetic field. A shock, passing at an oblique angle with respect to the field, increases the strength of the field and also changes its direction—in this case, by the same factor and through the same angle for both clumps.

Such a shock could produce the observed situation with the ~ 5 times lower field in the denser molecular clumps. If the initial configuration were a cloud with larger density on the inside, the angle by which the field is rotated by a shock depends on density, so that a smaller line-of-sight field in the higher density regions could be produced. Alternatively, if the initial configuration were a more uniform cloud, the density of the gas flowing downstream from the shock would increase as it cooled, again turning the field through an angle that depends on volume density. However, to obtain a reduction factor as large as 5 requires that the angle between the shock velocity and the magnetic field be specified to within a rather narrow range of angle, which is rather unlikely on an *a priori* basis.

As a final and rather farfetched possibility, we might compare the interstellar medium to the Sun. Inside a sunspot, smaller gas pressure is compensated for by magnetic pressure so that the total pressure is the same as it is outside the sunspot. Thus, low gas pressures correlate with high magnetic field strengths. In dense portions of the interstellar medium, where gas temperatures tend to be roughly the same, the corresponding statement would be that low gas densities correlate with high magnetic fields. This is equivalent to a cloud forming by expanding across the magnetic field lines as matter infalls along the field. Indeed, from the theoretical standpoint this is perhaps the only way that dense molecular clouds would be able to form spontaneously in a medium where magnetic pressure is not negligible. But why this should happen when gravity is negligible is difficult to comprehend.

V. SUMMARY

We have detected Zeeman splitting of the OH absorption lines toward Ori B and W22. Our result for Ori B agrees with the original detection of polarization by Verschuur and Turner (1970), and our derived field is consistent in magnitude, but not in direction, with that previously published by Crutcher and Kazes (1983). For W22 we derive a field of -11.0 ± 2.2 μG ($1\ \sigma$ error). This result refers to a dust cloud along the line of sight to W22 that has a rather typical density and temperature; the OH field toward W22 has also been detected by Crutcher and Kazes (1985), who interpret the results in detail.

The measured magnetic field strength is about $+9$ μG in all four OH velocity components of Cas A. The OH is located in small molecular clumps that have been studied at high-angular resolution in the H_2CO 6 cm line. Typical H_2 volume densities in these clumps are probably $\sim 3 \times 10^3$ cm^{-3}.

The molecular clumps are associated with H I clumps. In the H I clumps associated with two of the OH absorption components, the parallel component of the magnetic field is ~ 50 μG, ~ 5 times larger than in the denser molecular clumps themselves.

This is difficult to understand, because magnetic field strengths are expected to increase, not decrease, with increasing volume density. The possibility that the measured value of the field in the molecular clumps is much smaller than the total field because of tangling is unlikely, because the magnetic pressure in the clumps would then dominate the gas pressure, which would tend to keep the field from being tangled. A passing shock, moving obliquely to the magnetic field lines, could produce the observed situation, although this seems somewhat contrived. A farfetched possibility is that regions of low gas density tend to have higher magnetic field, in analogy with sunspots.

It is a pleasure to acknowledge extensive discussions with R. M. Crutcher concerning the sources Ori B and W22; W. M. Goss and T. L. Wilson concerning volume densities in Cas A; B. Elmegreen, P. Goldreich, T. Mouschovias, and F. Shu concerning theoretical aspects of magnetic fields in interstellar space; and, particularly, T. Troland concerning the observational interpretation in Cas A. This work was supported in part by the National Science Foundation to C. H.

REFERENCES

Barrett, A. H., Meeks, M. L., and Weinreb, S. 1964, *Nature*, **202**, 475.
Batrla, W., Walmsley, C. M., and Wilson, T. L. 1984, *Astr. Ap.*, **136**, 127.
Batrla, W., Wilson, T. L., and Martin-Pintado, J. 1983, *Astr. Ap.*, **119**, 139.
Bieging, J., and Crutcher, R. M. 1984, private communication.
Bregman, J. D., Troland, T. H., Forster, J. R., Schwarz, U. J., Goss, W. M., and Heiles, C. 1983, *Astr. Ap.*, **118**, 157.
Crutcher, R. M., and Kazes, I. 1983, *Astr. Ap.*, **125**, L23.
———. 1985, *Astr. Ap.*, submitted.
Davies, R. D., and Matthews, H. E. 1972, *M.N.R.A.S.*, **156**, 253.
de Jager, G., Graham, D. A., Wielebinski, R., Booth, R. S., and Gruger, G. M. 1978, *Astr. Ap.*, **64**, 17.
Field, G. B., Rather, J. D. G., Aannestad, P. A., and Orszag, S. A. 1968, *Ap. J.*, **151**, 953.
Goldsmith, P. F., Young, J. S., and Langer, W. D. 1983, *Ap. J. Suppl.*, **51**, 203.
Goss, W. M. 1968, *Ap. J. Suppl.*, **15**, 131.
Goss, W. M., Kalberla, P. M. W., and Dickel, H. R. 1984, *Astr. Ap.*, **139**, 317.
Heiles, C., and Troland, T. H. 1982, *Ap. J. (Letters)*, **260**, L23.
Henkel, C., Walmsley, C. M., and Wilson, T. L. 1980, *Astr. Ap.*, **82**, 41.
Kalberla, P. M. W., Schwarz, U., and Goss, W. M. 1985, in preparation.
Palmer, P., and Zuckerman, B. 1967, *Ap. J.*, **148**, 727.
Schwarz, U. J., Troland, T. H., Bregman, J. D., Goss, W. M., and Heiles, C. 1986, *Ap. J.*, **301**, 320.
Sherwood, W. A., and Wilson, T. L. 1981, *Astr. Ap.*, **101**, 72.
Troland, T. H., Crutcher, R. M., and Heiles, C. 1985, *Ap. J.*, **298**, 808.
Troland, T. H., and Heiles, C. 1982, *Ap. J.*, **252**, 179.
Verschuur, G. L. 1969, *Ap. J.*, **156**, 861.
Verschuur, G. L., and Turner, B. E. 1970, *Ap. J.*, **162**, 341.
Walmsley, C. M., and Ungerechts, H. 1983, *Astr. Ap.*, **122**, 164.
Weinreb, S., Barrett, A. H., Meeks, M. L., and Henry, J. C. 1963, *Nature*, **200**, 829.

CARL HEILES and MARY STEVENS: Astronomy Department, University of California, Berkeley, CA 94720